THE JOURNAL OF PHYSICAL CHEMISTRY C

Article

pubs.acs.org/JPCC

Single Molecule Surface-Enhanced Raman Spectroscopy: A Critical Analysis of the Bianalyte versus Isotopologue Proof

Alyssa B. Zrimsek,[†] Nolan L. Wong,[†] and Richard P. Van Duyne*[,†,‡,§]

[†]Department of Chemistry, [‡]Applied Physics Program, and [§]Department of Biomedical Engineering, Northwestern University, Evanston, Illinois 60208, United States

Supporting Information

ABSTRACT: Verification of single-molecule (SM) detection for surface-enhanced Raman spectroscopy (SERS) requires the use of two analytes via either the bianalyte or isotopologue approach. For both approaches, the preferential observation of the individual analytes over a combination of both analytes is used to conclude that SM detection has been achieved. Isotopologues are preferred because they have identical surface binding affinities and Raman cross sections, whereas bianalyte pairs typically do not. We conducted multianalyte SERS studies to investigate the limitations of the bianalyte approach. The bianalyte partners, Rhodamine 6G (R6G-d_0) and crystal violet (CV-d_0), were directly compared, while SM detection was verified (or disproved) using their corresponding isotopologues (R6G-d_4, CV-d_{12}). We found that the significant difference in counts between R6G and CV can provide misleading evidence for SMSERS. We then rationalized these results using a joint Poisson-binomial model with unequal detection probabilities and adjusted the relative concentrations of R6G and CV to achieve a comparable distribution of SMSERS counts. Using this information, we outlined the necessary considerations, such as accounting for the differences in molecular properties, for reliable SMSERS proofs. Moreover, we showed that multianalyte experiments at the SM level are achievable, opening the opportunity for new types of SM studies.

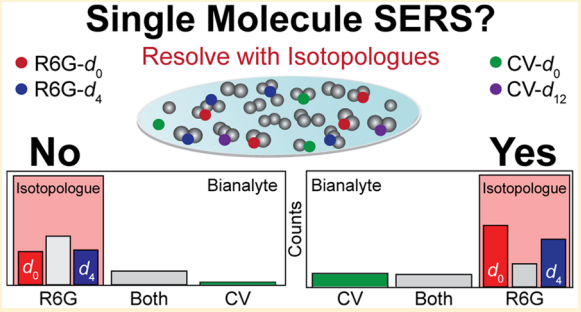

INTRODUCTION

Surface-enhanced Raman spectroscopy (SERS) is a powerful technique capable of the chemical and structural characterization of analytes near noble metal surfaces.[1−3] SERS is useful for elucidating the mechanisms of electrochemical,[4,5] heterogeneous catalytic,[6] and other surface chemical reactions. In 1997, a renewed interest in SERS was sparked by the first observations of single-molecule (SM) sensitivity.[7,8] Highly sensitive and selective, SMSERS facilitates the exploration of local environment heterogeneity and molecular properties typically obscured by ensemble averaging.

Initial acceptance of SMSERS as a viable technique was impeded by the complexity of proving SM detection. In fluorescence spectroscopy, SM sensitivity can be unequivocally proven through the observation of photon antibunching (i.e., the fact that a SM cannot emit two fluorescence photons simultaneously).[9−11] Antibunching is not possible for SMSERS because the lifetime of Raman scattering is too short at $<10^{-14}$ s. It is also common in SM fluorescence to rely on ultralow analyte concentrations. The analyte is diluted such that one or fewer molecules are present in the probe volume. The exclusive use of ultralow concentrations for SMSERS, unfortunately, is inadequate. The molecules must be adsorbed to nanoparticle surfaces. This means estimating the number of molecules being probed is a convolution of the analyte and nanoparticle concentrations, the adsorption efficiency of the molecules to the nanoparticles, the positions of the molecules relative to the plasmonic hotspots, and the number of nanoparticles in the probe volume. Along with ultralow concentrations, early studies often used strong fluctuations in intensity and spectral shape, spectral wandering, and blinking as evidence for SM detection.[12−15] Although these fluctuations are characteristic behaviors of SMs, they have also been observed at the few-molecule level[16] and only provide indirect evidence for SMSERS. Consequently, strategies began to combine ultralow concentrations with statistical analysis to more rigorously support claims of SM detection.[7,17−19]

At very low molecular coverage, the SERS events or number of molecules detected per spectrum will follow a Poisson distribution. Due to a greater than 10-fold signal variability between SM events, however, distinguishing between intensities that correspond to 1, 2, or 3 molecules is not feasible.[16,20,21] Furthermore, a reliable Poisson analysis would require a minimum of 10000 sample events, which is generally an impractical feat for SMSERS.[20] As a result of these limitations, the bianalyte[22−24] and isotopologue[16,25−27] approaches were developed to demonstrate SM detection. Both approaches involve dosing a SERS-active substrate with an

Received: January 19, 2016
Revised: February 10, 2016
Published: February 11, 2016

DOI: 10.1021/acs.jpcc.6b00606
J. Phys. Chem. C 2016, 120, 5133−5142

equimolar mixture of two analytes. The bianalyte approach uses two different analyte molecules, whereas the isotopologue approach uses an analyte and an isotopically labeled version of that analyte. The key advantage of isotopologues is that the two analytes will have identical surface binding chemistries and overall Raman cross sections. To verify SMSERS, events with the individual analytes should be preferentially observed over events with both analytes.

A combined Poisson and binomial distribution was proposed for the isotopologue method to model the number of molecules of isotopologue 1 and isotopologue 2 detected per spectrum.[16] The probability of SMSERS detection is represented by the Poisson distribution, and the probability that the observed event will correspond to either isotopologue 1 or isotopologue 2 is represented by a binomial distribution (assuming a 50:50 probability of either isotopologue 1 or 2 as the identity of a given molecule). The joint probability is summarized as follows:

$$P(n_1, n_2, \alpha) = \frac{e^{-\alpha}}{n_1! n_2!}\left(\frac{\alpha}{2}\right)^{(n_1+n_2)} \quad (1)$$

where n_1 and n_2 are the number of molecules of isotopologues 1 and 2 detected in the SER spectrum, respectively, and α is the estimated number of molecules adsorbed per nanoparticle aggregate. P is the probability that n_1 isotopologue 1 and n_2 isotopologue 2 molecules at α-coverage will be detected for a given spectrum. From this model, Dieringer et al. proposed a theoretical SM level threshold at $\alpha = 1$ (i.e., a mean of 1 molecule per nanoparticle aggregate).[16] This means that at least 76% of the spectra must indicate the character of a single analyte over a combination of both analytes in order to prove SM sensitivity.

The above analysis is problematic for bianalytes because the analytes typically have different binding affinities and Raman cross sections. As a consequence, the isotopologue method is preferred, but it is subject to practical limitations such as cost and synthetic complexity. Moreover, the isotopologues must have a significant, observable spectral peak shift to allow accurate identification of the two isotopologues. Under these limitations, the bianalyte approach can be experimentally unavoidable.

The impact of molecular diffusion and adsorption to nanoparticles in colloidal solutions on SMSERS has also been investigated for isotopologues.[28] Due to competition between molecular diffusion and adsorption, the dilution procedure used for sample preparation can drastically alter the homogeneity of molecular coverage on the nanoparticles. This can lead to the artificial appearance of SM detection when, in reality, multiple molecules are present. Darby et al. advise premixing the analytes and using half−half dilutions in lieu of large dilution factors. Similarly, it is critical that we elucidate the necessary experimental considerations to convincingly demonstrate SM sensitivity with the bianalyte method.

To probe the limitations of the bianalyte approach for SMSERS, we undertake the first multianalyte SMSERS experiment. We dosed Ag colloids with two pairs of isotopologues: Rhodamine 6G (R6G-d_0, R6G-d_4) and crystal violet (CV-d_0, CV-d_{12}). The bianalyte pair (R6G and CV) can be directly compared, while simultaneously proving SMSERS using their corresponding isotopologues as an internal standard. From these results and a detailed discussion of a joint Poisson-binomial model under conditions of unequal analyte detection, we outline the considerations necessary for accurate implementation of SMSERS proofs. Furthermore, we demonstrate that multianalyte studies at the SM level are a viable approach for future investigations, such as monitoring SM chemical reactions.

EXPERIMENTAL SECTION

SMSERS Sample Preparation. The borohydride-reduced Ag colloids were synthesized following a previously reported procedure with slight modification.[22] A detailed procedure for the nanoparticle synthesis is provided in the Supporting Information. After synthesis, the colloids were concentrated by centrifugation for the SMSERS experiments. In a centrifuge tube, 1 mL of as-prepared colloids was centrifuged for 5 min at 5000 rcf, followed by removal of the supernatant. This process was repeated 4 more times (i.e., total 5 mL of colloids into 1 sample), and the colloids were dispersed to a final volume of 100 μL (~50 fold increase in concentration) with Millipore water (18.2 MΩ cm) by vortexing for 30 s. In accordance with the dilution procedure described previously, to avoid surface coverage nonuniformity, we did not employ large dilution factors.[28] Instead, we added 50 μL of the dilute dye mixtures to the concentrated colloids and vortexed for 1 min to thoroughly mix. The concentrations of the multianalyte and bianalyte dye mixtures varied for each data set (Table 1). These dyes included Rhodamine 6G (R6G-d_0, Sigma), crystal violet (CV-d_0, Sigma), and their isotopologues (R6G-d_4 and CV-d_{12}, custom synthesis as previously described).[16,27] The colloid/dye mixtures were allowed to incubate in a N_2 environment for 2 h. Glass coverslips (25 mm, no. 1.5) were piranha cleaned (3:1 H_2SO_4/30%H_2O_2) and base treated (5:1:1 H_2O/NH_4OH/30% H_2O_2), and then dropcast with 10 μL of the colloid/dye mixture and dried with a N_2 gun. This step was repeated twice (total drop volume of 20 μL) to ensure adequate nanoparticle coverage for scanning.

Table 1. Individual Component and Total Solution Concentrations

Data Set	Concentration (M)				
	R6G-d_0	R6G-d_4	CV-d_0	CV-d_{12}	Total
A	1×10^{-7}	–	1×10^{-7}	–	2×10^{-7}
B	1×10^{-8}	–	1×10^{-8}	–	2×10^{-8}
C	5×10^{-8}	5×10^{-8}	5×10^{-8}	5×10^{-8}	2×10^{-7}
D	5×10^{-9}	5×10^{-9}	5×10^{-9}	5×10^{-9}	2×10^{-8}
E*	1×10^{-9}	1×10^{-9}	1×10^{-9}	1×10^{-9}	4×10^{-9}
F	1×10^{-10}	1×10^{-10}	4×10^{-9}	4×10^{-9}	8.2×10^{-9}

*Data Set E is provided in Figure S4.

Instrumentation and Scans. The SMSERS substrates were mounted in a custom-built flow cell under a positive pressure of N_2 for the entire duration of data collection to minimize photodegradation. A detailed description of the instrumentation and a schematic of the scanning setup (Figure S1) are provided in the Supporting Information. The SMSERS substrates were scanned with a piezo-controlled stage (E-710 Digital PZT) with a step size of 2 μm in the x- and y-directions. The step size was chosen to be larger than the laser spot size (~1 μm^2) to limit exposure of the molecules to the laser during long scans. At each step of the scan, a spectrum was collected for 1−5 s with an incident power of 6−7 μW. Only events that were clearly distinguishable as R6G-d_0, R6G-d_4, CV-d_0, CV-d_{12},

DOI: 10.1021/acs.jpcc.6b00606
J. Phys. Chem. C 2016, 120, 5133−5142

or a combination thereof were counted. Spectra with spurious peaks which were attributed to R6G or CV photodecomposition products or carbonaceous species were not counted.[18,29] It should be noted that many of the spectra in the scans were blank. This is the result of the low concentrations used and the typically small percentage of SMSERS-active nanoparticles.[30] As a result, multiple scans were run to build each data set.

RESULTS AND DISCUSSION

Bianalyte and Multianalyte SMSERS. We pursued multianalyte studies to investigate the limitations of the bianalyte method for SMSERS. Figure 1 shows example

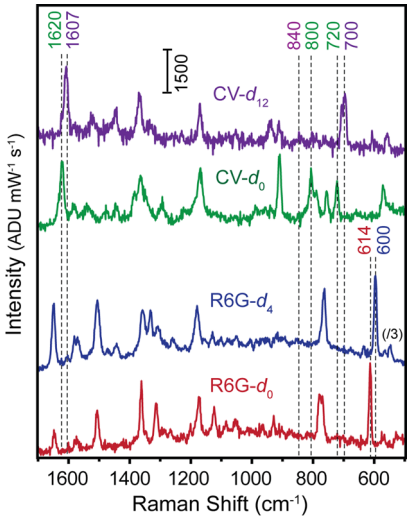

Figure 1. Example single-molecule SER spectra of Rhodamine 6G (R6G-d_0 and R6G-d_4) and crystal violet (CV-d_0, and CV-d_{12}) collected from Ag colloids dosed in a dilute mixture of all four analytes. Only the character of each individual analyte is observed. Characteristic modes used for the identification of each analyte are indicated on the spectra.

SMSER spectra of R6G, CV, and their corresponding isotopologues collected from Ag colloids incubated with a dilute mixture of all four analytes. R6G-d_0 has a strong, isotopically sensitive mode at 614 cm^{-1}, which upon deuteration of the phenyl moiety (R6G-d_4) shifts to 600 cm^{-1}.[16] A histogram tabulating the peak frequencies for the 600 cm^{-1} region mode of R6G and additional spectra are provided in Figure S2. As discussed in previous literature,[27] upon deuteration of CV-d_0 to CV-d_{12}, many subtle changes in peak frequencies occur. The most prominent feature is the shift of the 1620 cm^{-1} band in CV-d_0 to 1607 cm^{-1} in CV-d_{12}. While this mode can be used for differentiating the CV isotopologues, it can be obscured by R6G modes in the same spectral region. A convenient point of contrast between CV and R6G are the 630 to 750 cm^{-1} and 780 to 900 cm^{-1} regions, in which R6G is featureless. In these regions, CV-d_0 has bands at 720 and 800 cm^{-1}, and CV-d_{12} has bands at 700 and 840 cm^{-1}. Throughout the rest of this study, the bands between 600 and 800 cm^{-1} and 1600−1630 cm^{-1} were used to differentiate the SMSER spectra for the various analytes. Example multianalyte spectra showing instances of 3 or 4 analytes are shown in Figure S3.

Data Sets A and B (Figure 2) correspond to two bianalyte experiments completed with equimolar mixtures of R6G-d_0 and CV-d_0. In Data Set B, order of magnitude lower concentrations were used compared to those in Data Set A (see Table 1). The CV/R6G column in the bianalyte histograms accounts for any instances in which both R6G-d_0 and CV-d_0 were detected in the SER spectrum. In Data Set A, 76% of the spectra showed individual analyte character of either R6G or CV, but not both. In Data Set B, 95% of the spectra showed individual analyte character.

Recall from Equation 1 that to satisfy a theoretical SM level threshold at $\alpha = 1$, or on average one molecule per spectrum, at least 76% of the spectra must indicate individual analyte character. On first glance, Data Sets A and B satisfy this threshold, suggesting SM level coverage in both cases. However, we found that the counts for R6G were an order of magnitude higher than those of CV for both Data Sets A and B (∼14 and ∼11 times, respectively). The observation of this trend over hundreds of counts suggests that the detection probabilities of CV and R6G are significantly different. The large discrepancy in counts between R6G and CV is attributed to differences in their adsorption affinities and resonance Raman cross sections. Different binding affinities will result in unequal molecular coverage on the SERS substrate, favoring the detection of the analyte with the stronger affinity. Clearly, the assumption in Equation 1 of a 50:50 detection probability for CV and R6G is not valid. Therefore, Data Sets A and B may not actually satisfy the theoretical threshold for SM detection. This will be addressed in a subsequent section, but first, to experimentally verify whether or not these data sets are at the SM level, we conducted analogous multianalyte experiments.

Data Sets C and D provided in Figure 2 correspond to multianalyte experiments conducted under identical conditions to those for Data Sets A and B, respectively. For the multianalyte studies, the Ag colloids were dosed with equimolar dye mixtures of all four analytes. The individual concentrations of R6G-d_0 and RG6-d_4 (or CV-d_0 and CV-d_{12}) in Data Set C sum to the total concentration of R6G-d_0 (CV-d_0) dosed onto the nanoparticles in Data Set A. This dosing scheme was repeated for Data Sets D and B at their order of magnitude lower concentrations. By following identical procedures for sample preparation and maintaining the same overall concentration, we are able to compare the purely bianalyte experiments with their analogous multianalyte experiments. The multianalyte studies allow us to distinguish, for an individual analyte's SERS events in the bianalyte approach (i.e., R6G or CV), between counts that have individual or both isotopologue character. As expected, if we sum all of the R6G-d_0/d_4 events and all of the CV-d_0/d_{12} events in the multianalyte experiments, R6G is still preferentially observed by an order of magnitude over CV. For the multianalyte histograms, the CV/R6G column accounts for all possible combinations of a R6G isotopologue with a CV isotopologue, including instances of 3 or 4 analytes.

Upon examination of the isotopologue distributions in Data Set C, we found that spectra containing either both R6G-d_0/d_4 or both CV-d_0/d_{12} were observed more frequently than their respective individual isotopologue spectra. Despite 76% of the spectra in Data Set A showing individual analyte character, the isotopologue internal standard in Data Set C demonstrates that these two analogous experiments were actually at the few-molecule level. In Data Set D, in which the concentrations were lowered by an order of magnitude, we found that individual R6G-d_0 and R6G-d_4 spectra were observed preferentially over the combination of both isotopologues. The same held true for the CV isotopologues. Thus, the circumstantial evidence of SMSERS for Data Set B was shown, via isotopologue internal

DOI: 10.1021/acs.jpcc.6b00606
J. Phys. Chem. C 2016, 120, 5133−5142

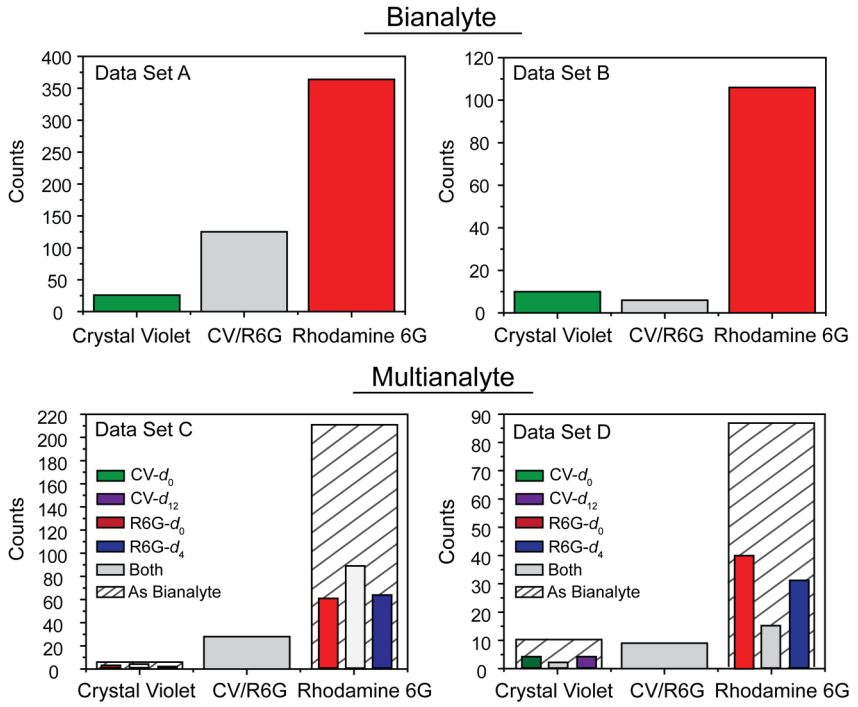

Figure 2. Histograms of counts for bianalyte SERS experiments conducted with CV-d_0 and R6G-d_0 in Data Set A at 1×10^{-7} equimolar concentration and Data Set B at 1×10^{-8} equimolar concentration. The CV/R6G column in Data Sets A and B accounts for any instances when both R6G-d_0 and CV-d_0 were detected in the SER spectrum. Data Sets C and D are analogous multianalyte experiments to Data Sets A and B, respectively, conducted at an identical overall concentration but with the concentration divided between the isotopologue pairs: CV-d_0, CV-d_{12}, R6G-d_0, and R6G-d_4. See Table 1 for further concentration details. For Data Sets C and D, the CV/R6G column accounts for all possible combinations of a R6G isotopologue with a CV isotopologue, including instances of 3 or 4 analytes. The columns filled with slashed lines are the sum of the individual events within the column, displaying the multianalyte data sets as though they were a bianalyte experiment for direct comparison. In all of the data sets, R6G was observed an order of magnitude more times than CV. It was determined using the isotopologue internal standards that Data Sets A and C are at the few-molecule level, while Data Sets B and D are at the single-molecule level.

standards, to be correct. It should be noted that while the individual isotopologue spectra for CV were preferentially observed over the presence of both isotopologues, the overall counts for CV were low. For a more rigorous demonstration of SMSERS, more counts are needed.

In summary, we experimentally verified that the largely different detection probabilities of R6G and CV can misleadingly imply SM detection, when it has not actually been achieved. To provide further evidence that the trends we observed were reproducible, we completed a third multianalyte experiment (Data Set E, Figure S4), at an additional order of magnitude lower concentration compared with Data Set D. Following the same trend, the observed number of counts for R6G was an order of magnitude higher than that for CV. This verifies that the trends in bianalyte behavior were reproducible for equimolar concentrations spanning 2 orders of magnitude (1×10^{-7} to 1×10^{-9} M). In the following sections, the influence of the Raman cross sections and binding affinities will be addressed, and the appropriate interpretation of bianalyte proofs will be examined.

Signal Intensity Variance, Binding Affinities, and Detection Probabilities. The detection probabilities for each analyte are controlled by their Raman cross sections, binding affinities, and solution concentrations. First, we consider the importance of the Raman scattering cross sections for the bianalyte approach. The enhancement factor for Ag colloids, the most commonly utilized substrate for SMSERS, varies from hotspot to hotspot.[30−32] Also, the hotspot enhancement has been demonstrated to follow a long-tail distribution.[20,22] From a detection standpoint, this means that there is an effective region of the hotspot which can provide sufficient enhancement for the molecule to be detected above the noise. Therefore, the higher the analyte's cross section, the larger this effective region, and the more available sites the analyte has to be detected. As a result, we believe analytes with higher cross sections will have a larger variance in signal intensity between SM events than those with smaller cross sections.

The Raman cross section of R6G at 3.26×10^{-24} cm^2/(molecule sr) is an order of magnitude greater than that of CV at 2.85×10^{-25} cm^2/(molecule sr) for the 614 and 1620 cm^{-1} modes, respectively.[33,34] We predicted that this fairly large difference in cross sections would lead to unequal signal variances between R6G and CV, with R6G having the larger variability in SERS intensities between events. Using the multianalyte data sets found to be at the SM level [Data Sets D, E, and F (Figures 2, S4, and 5A)], we examined the relative intensities for the 1600 cm^{-1} region modes of CV-d_0 and CV-d_{12} and the 600 cm^{-1} region modes of R6G-d_0 and R6G-d_4. All spectra were normalized for excitation power and acquisition time. Figure 3A provides example spectra for both R6G and CV, highlighting the large variability in signal intensity observed.

In Figure 3B, the histogram of the relative intensities is plotted on a logarithmic scale. We found that the relative intensities spanned almost 3 orders of magnitude for R6G and just over 2 orders of magnitude for CV. As predicted, from the fits of the histograms, we found that the variances for R6G and

DOI: 10.1021/acs.jpcc.6b00606
J. Phys. Chem. C 2016, 120, 5133−5142

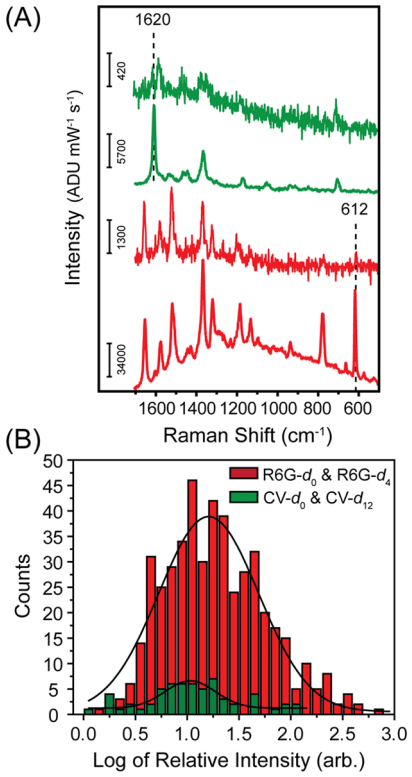

Figure 3. (A) Example SMSER spectra of R6G (red) and CV (green) showing the large variation in intensities observed between different SM events. (B) A histogram of the relative peak intensities, plotted on a logarithmic scale, for the 1600 cm^{-1} region mode of CV-d_0 and CV-d_{12} and the 600 cm^{-1} region mode of R6G-d_0 and R6G-d_4. The distribution of relative intensities for R6G spanned almost 3 orders of magnitude, while that of CV spanned just over 2 orders of magnitude. The variances for the CV and R6G intensities were found to be unequal with a $p < 0.001$ (F-test).

CV were unequal with a $p < 0.001$ (F-test). The unequal variances highlight the importance of considering the Raman scattering cross section when using the bianalyte approach. Even if the analytes are present at equal coverage, the analyte with the weaker cross section may not be equivalently detectable above the noise, leading to different detection probabilities. As a consequence, it is preferential to choose bianalyte partners with cross sections within an order of magnitude of each other. It should be noted that while steps were taken to limit photodegradation, we cannot eliminate the possibility of differences in photostability between R6G and CV, which can contribute to the unequal variances in signal intensity.

Next, we consider the impact of the analyte binding affinities. In the case of equivalent analyte Raman cross sections and equimolar solution concentrations, the analyte with the stronger binding affinity will have a higher surface coverage and therefore a higher detection probability. Our various attempts to quantify the binding affinities of CV and R6G on Ag have demonstrated that this is a challenging task. While it is clear that both the Raman cross sections and binding affinities will influence the relative analyte detection probabilities, the relative contributions of the two aforementioned properties remain unclear and are analyte-dependent. We attempted to examine this by devising an expression relating the detection probability to the cross section and binding affinity, but the unknown enhancement factor distribution for the polydisperse and randomly aggregated Ag colloids complicated this task. We believe, however, that it is possible to correct for differences in detection probability by adjusting the ratio of the analyte concentrations. This will be addressed in subsequent sections.

Joint Poisson-Binomial Model. As discussed previously regarding the bianalyte approach, the detection probabilities of the two analytes will not be equivalent in most cases. To better understand the implications of this on the interpretation of bianalyte proofs, we generalized the proposed joint Poisson-binomial probability in Equation 1 to the bianalyte method:

$$P(n_1, n_2, \alpha, \beta) = \frac{e^{-\alpha}}{n_1! n_2!}[\alpha\beta]^{n_1}[\alpha(1-\beta)]^{n_2} \quad (2)$$

where α is the average number of molecules per scan pixel (each pixel corresponds to one spectrum), and n_1 and n_2 are the number of analyte 1 and analyte 2 molecules detected in the SER spectrum, respectively. P is the probability that n_1 analyte 1 and n_2 analyte 2 molecules at α-coverage will be detected for a given spectrum. The probability that a given molecule detected in the spectrum corresponds to analyte 1 is designated with an empirical variable β (value between 0 and 1; $\beta = 0.5$ for the isotopologue method which has a 50:50 ratio). The value of β is a function of the binding affinities, concentrations of analytes 1 and 2, and Raman cross sections. While it remains a challenge to develop a rigorous expression combining all of these factors, we can still examine how the value of β impacts the bianalyte method's validity in the context of this model.

We propose using the percentage of SER spectra with individual analyte character to characterize whether or not SM levels have been achieved for a bianalyte experiment. As visualized in Figure 4A, this criterion is defined as the sum of the individual analyte 1 and analyte 2 counts, divided over the total spectral counts (analyte 1 + analyte 2 + both). For this criterion, spectra containing zero molecules are excluded. As can be expected, as the percentage of individual character increases, there is a higher probability of SM detection. For the remainder of this discussion, all calculated parameters from Equation 2 were computed using MATLAB for up to 10 molecules of either analyte 1 or analyte 2 contributing to a given event. Beyond 10 molecules per spectrum, when $\alpha < 4$, the probability calculated from Equation 2 is negligible.

Figure 4B depicts the calculated percentage of SER spectra with individual character from Equation 2, plotted as a function of various α and β values. Figure 4 (panels C and D) shows the associated contours plotted as functions of α and β, respectively. In Figure 4C, it is evident that as the overall coverage of molecules increases (i.e., as α increases), the percentage of SER spectra with individual character decreases (i.e., less likely to achieve SM detection). However, as the probability of detecting analyte 1 deviates from 50% (i.e., when $\beta \neq 0.5$) and α is held constant, the percentage of SER spectra with individual character increases (Figure 4D). Essentially, the higher probability of detecting analyte 1 (or 2) leads to a greater number of individual analyte 1 (or 2) counts, resulting in a "skewed" increase in the percentage of SER spectra with individual character. With respect to interpreting the bianalyte experiments, this means that when the binding affinities and Raman cross sections differ significantly between the two analytes (and the analytes are dosed at equimolar concentrations), a larger (smaller) percentage of SER spectra with individual (both) character is required to demonstrate SM levels.

DOI: 10.1021/acs.jpcc.6b00606
J. Phys. Chem. C 2016, 120, 5133−5142

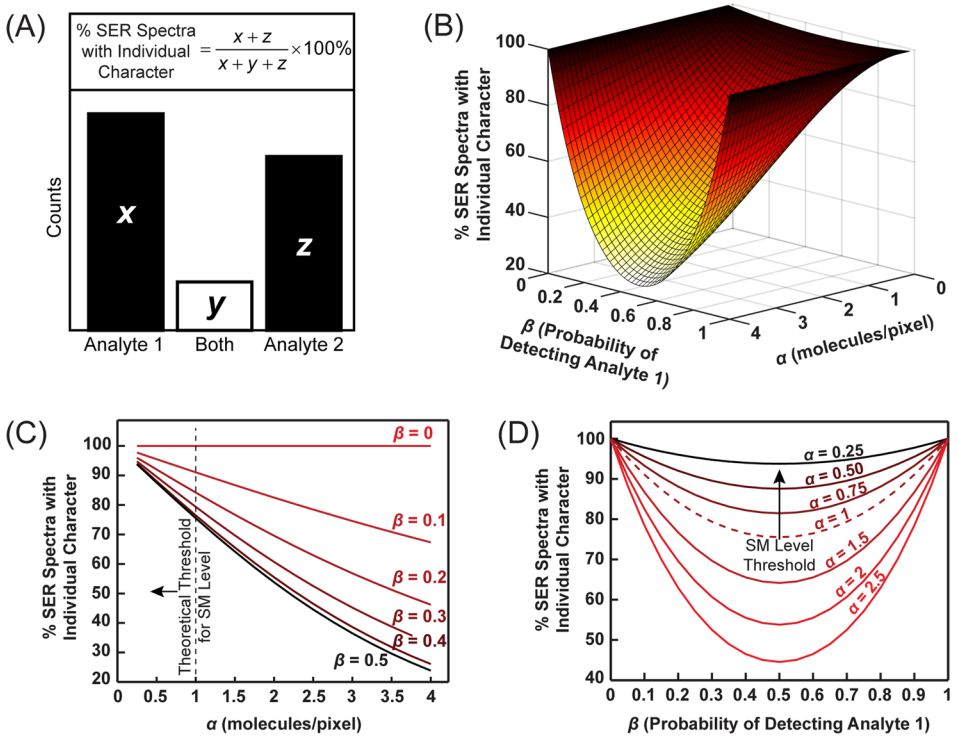

Figure 4. (A) Schematic demonstrating how the percentage of SER spectra with individual analyte character is defined with respect to the experimentally obtained histograms. (B) Theoretically calculated percentage of SER spectra with individual character from Equation 2, plotted as a function of the average number of molecules per scan pixel (α) and the probability that analyte 1 will be detected (β). Note that the probability that analyte 2 will be detected corresponds to (1-β). All calculations were done with MATLAB for up to 10 molecules of either analyte 1 or 2. (C) Contours selected from (B), plotted against α. (D) Contours selected from (B), plotted against β. The theoretical threshold shown is defined as the point at which on average one molecule is detected per scan pixel.

As mentioned earlier during the experimental discussion, a proposed definition for the theoretical SM level threshold is the point at which $\alpha = 1$. This corresponds to, on average, one analyte being detected per scan pixel and is visualized in Figure 4 (panels C and D) with dashed lines. When the probability of detecting analyte 1 is 50% ($\beta = 0.5$), at least 76% of the SER spectra must exhibit individual character in order to reach SM levels. On first glance, both bianalyte Data Sets A and B satisfied this requirement. However, as mentioned before, the discrepancy in counts between R6G and CV indicates that the probabilities of detecting CV and R6G (i.e., β) have shifted far from 50%. Assuming a $\beta = 0.1$, close to the ratio of counts between CV and R6G in our data sets, 91% of the SER spectra must exhibit individual character in order to reach SM levels. This theoretical threshold fits well with the experimental results presented earlier: Data Set A (76% individual character) was not at the SM level based on the isotopologue internal standard, whereas Data Set B (95% individual character) was at the SM level.

In order to explicitly evaluate whether or not the theoretical SM level threshold is met, an approach to estimate the values of α and β for an experiment is desired. The probabilities of detecting analytes 1 and 2 should be related to the relative number of counts in the individual analyte 1 versus 2 columns of the histogram. However, there are 4 variables that must be evaluated simultaneously: the relative number of individual analyte 1 versus analyte 2 counts, the total number of counts with both analytes, α, and β. It is worth noting here that utilizing the relative intensities of analyte 1 and analyte 2 in an average spectrum of all events to estimate β (as opposed to the relative number of analyte 1 versus 2 counts) is unreliable. See the Supporting Information for further discussion.

Figure S6 displays a pictorial method to determine α and β, given the percentages of SER spectra with individual analyte 1 and individual analyte 2 character. Inevitably, values of α and β must be calculated from the model defined by Equation 2. This was accomplished by computing individual analyte 1 and analyte 2 percentages for a variety of α and β and locating the point at which the experimental individual analyte 1 and 2 percentages, α, and β values simultaneously match. The calculated values for Data Sets A ($\alpha = 2.06$, $\beta = 0.15$) and B ($\alpha = 0.52$, $\beta = 0.10$) align well with the experimental conclusions. The 5% difference in β-values for the two data sets is primarily a result of insufficient counts (thousands are needed for a more exact value). This highlights the preference to work in terms of "β-regimes", those close to $\beta = 0.5$ (from 0.35 to 0.65) and those far from $\beta = 0.5$ (0 to 0.35 and 0.65 to 1). The β-regime close to $\beta = 0.5$ is defined from 0.35 to 0.65 because in this range the percentage of individual character spectra required for SM levels ($\alpha = 1$) only fluctuates by ~1%. Outside of this range, the SM level threshold changes drastically for different β values (see Figure 4D). Given the higher thresholds that must be met at β-regimes far from 0.5, it is experimentally preferable to employ one of the following strategies: (1) use isotopologues, (2) adjust analyte concentrations to enter a β-regime close to 0.5, or (3) select bianalyte partners with nearly identical molecular properties.

It is critical to emphasize that the model summarized by Equation 2 corresponds to the ideal case, and that it is challenging to exactly match the experimental results to the model without thousands of data points. Dieringer et al.

DOI: 10.1021/acs.jpcc.6b00606
J. Phys. Chem. C 2016, 120, 5133−5142

discussed earlier that this model does not account for the fact that the SER enhancement factor is nonuniform across the substrate surface, lowering the probability of finding both analytes in a hotspot.[16] In addition, the model assumes no spatial correlations between analyte-surface binding events (i.e., no dimerization or preferential clustering of analyte molecules). If the analytes preferentially cluster, this can increase the probability of detecting multiple same-analyte molecules clustered in a hotspot. This clustering effect can be experimentally minimized by selecting analytes that exhibit minimal dimerization at low concentrations, and by following the dilution procedures described by Darby et al.[28] Finally, this model is only valid when the experimental method involves spatial or temporal sampling to follow a Poisson distribution.

SMSERS with Unequal Analyte Concentrations. As addressed in the previous section, the ideal condition for a SMSERS proof is to have equal detection probabilities for both analytes. One approach to account for differences in detection probability is to adjust the concentrations of the two analytes. We experimentally observed in all previously discussed data sets that R6G is preferentially detected over CV by roughly an order of magnitude. On the basis of this information, we determined that to achieve comparable counts for R6G and CV, the CV concentration needed to be at least a factor of 10 higher than the R6G concentration. The next step was to ensure that the CV and R6G concentrations were set at or below the coverage threshold required for SM levels. CV was demonstrated in our experiments to be in the few-molecule regime at 1×10^{-7} M (Data Sets A and C). Therefore, we set the CV concentration well below this threshold at 4×10^{-9} M and lowered the R6G concentration further to 1×10^{-10} M. The histogram collected with this dilute mixture of all 4 analytes is shown in Figure 5A as Data Set F. The R6G counts are only 1.2 times higher than the CV counts, instead of an order of magnitude. With a β-regime close to 0.5 and 94% individual character observed for the bianalyte interpretation, Data Set F is at the SM level. The isotopologue internal standards provide further evidence to support this conclusion. In Figure 5B, we provide a 100 × 82 μm reconstructed scan map displaying the locations and identities of the molecule(s) detected. Each pixel of the map is 2 × 2 μm, as described in the Experimental Section. From this map, it is clear that the various molecules are spread out and randomly dispersed across the surface. Thus, we were able to demonstrate that by altering the concentration ratios of the bianalyte molecules, we achieved SMSERS and equivalent counts of R6G and CV.

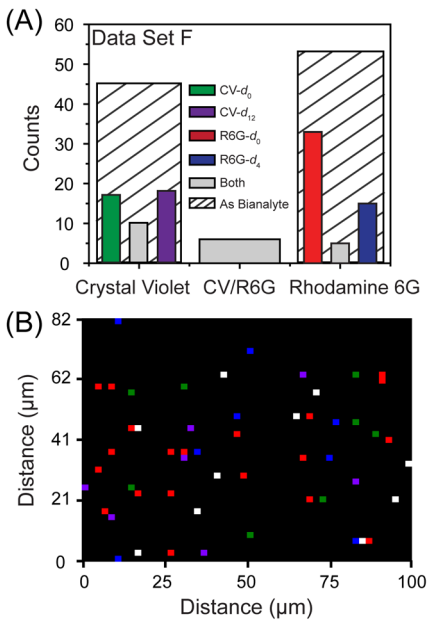

Figure 5. (A) Histogram of counts for a multianalyte experiment conducted with Ag colloids dosed with a 40 times higher CV concentration compared to the R6G concentration (4×10^{-9} M and 1×10^{-10} M, respectively). Comparable counts were observed for both CV and R6G. (B) 100 × 82 μm reconstructed scan map showing the locations of the molecules for one scan of Data Set F. A spectrum was collected at each 2 × 2 μm pixel of the map. The molecular identity is indicated by the color in (A).

Thresholds for SMSERS. Another important consideration often overlooked is that the bianalyte and isotopologue proofs generally constitute "single analyte" and "single isotopologue" proofs. When at SM level coverage, it is possible that a single analyte spectrum may actually correspond to 2, 3, 4, or more molecules of the same analyte. This issue can be visualized in Figure S7A. The percentage of single molecule events is defined as the fraction of individual analyte 1 or 2 spectra that actually correspond to single molecules. In Figure S7B, the calculated (from Equation 2) percentage of single molecule events is plotted for various values of α and β. In accordance with the model, for $\alpha = 1$ and $\beta = 0.5$, only 77% of the individual analyte 1 or 2 counts correspond to SM events. The remaining counts correspond to events with 2 or more molecules. Thus, for the earlier defined $\alpha = 1$ SM threshold, while most of the individual counts correspond to single molecules, there remains a significant probability that an individual analyte spectrum corresponds to multiple molecules of the same analyte. Furthermore, when the probabilities of detecting analytes 1 and 2 shift away from a 50:50 ratio, the analyte with a higher (lower) probability of detection has a lower (higher) percentage of actual SM events.

While we are currently unable to experimentally verify if a single analyte spectrum corresponds to 2 or more molecules, the multianalyte experiments allowed us to resolve instances of 3 or 4 molecules in a single spectrum. At the few-molecule level (Data Set C), the occurrences of spectra indicating the presence of 3 or 4 analytes were 7% and 3%, respectively. Example spectra are provided in Figure S3. Moving to SM level coverage (Data Sets D, E, and F), we found no instances of spectra with character from all 4 analytes, but 1% of the spectra still showed character of 3 analytes. It should be noted, due to the discrepancy in counts between R6G and CV, these results likely underestimate the number of events with three or more molecules. These results demonstrate that SERS events with two or more molecules can contribute measurably to the total counts.

The non-negligible probability of simultaneously observing two or more same-analyte molecules highlights the importance of defining more rigorous thresholds for SM detection. A way to define this rigorous threshold is the point at which we have 95% confidence that an individual analyte's SER spectrum corresponds to a single molecule. By calculation from Equation 2, for any β-value, at least 95% single molecule events for both analytes will be achieved at $\alpha = 0.10$ or less (i.e., at least 99% SER spectra with individual character). In the β-regime close to $\beta = 0.5$, 95% single molecule events for both analytes is reached at $\alpha = 0.16$ (i.e., 96% SER spectra with individual character). In practice, the SM threshold set at $\alpha = 1$ may be sufficient, such

DOI: 10.1021/acs.jpcc.6b00606
J. Phys. Chem. C 2016, 120, 5133−5142

as when proving that a SERS substrate is capable of SM sensitivity. The second, more rigorous, threshold is best geared toward experiments which require demonstration that a single molecule is indeed being monitored. The two defined SM thresholds are summarized for each β-regime in Table 2.

Table 2. Thresholds for Single-Molecule Level Detection

Defined SM level threshold	α	β-regime	% SER spectra with individual character
On average 1 molecule per spectrum	1	0 to 0.35	91.1
	1	0.35 to 0.65	76.0
	1	0.65 to 1	91.1
95% of individual analyte SER spectra correspond to SMs	0.1	0 to 0.35	99.0
	0.16	0.35 to 0.65	96.2
	0.10	0.65 to 1	99.0

Considerations for the Bianalyte Approach. Ideally, isotopologues will be used to prove SM detection for future SMSERS investigations. Isotopologues do not suffer from the limitations of bianalyte partners. When this is not a viable strategy, however, optimal bianalyte partners should be selected. The analytes should have clear spectral differences for unambiguous identification of the individual analytes and their mixtures. Next, the chosen bianalyte partners should have comparable Raman scattering cross sections (same order of magnitude) because even under the condition of equivalent molecular coverage, significantly unequal cross sections will lead to different detection probabilities. Another important consideration is that the selected analytes are reasonably photostable.[35] If one bianalyte partner degrades more readily, the distribution of SERS events could be potentially skewed in favor of the more stable analyte.

Despite careful selection of the bianalyte partners, significant differences in binding chemistries may remain. To efficiently correct for differences in molecular coverage, the relative adsorption affinities of the two analytes to the SERS substrate should be known or estimated. Then, if the analytes have similar Raman cross sections, the molecular coverage can be easily corrected by adjusting the analyte concentrations. The proper strategy for adjusting the concentrations must be assessed on a case-by-case basis because the molecular properties are dependent upon the bianalyte pair selected. For example, whether the molecules bind kinetically or thermodynamically can influence the procedures necessary for sample preparation (e.g., length of incubation). Once these considerations have been made, a concentration for each analyte can be selected. During sample preparation, it is also very important to follow the dilution procedures described by Darby et al., to avoid nonuniformity in nanoparticle coverage in colloidal solutions.[28] Furthermore, to employ the theoretical thresholds defined in Table 2, the experimental procedure should involve spatial or temporal data collection to ensure that the joint Poisson-binomial model (Equation 2) is valid. Due to the large number of variables in SMSERS investigations, the experimental details for sample preparation and data collection should always be clearly stated, as these procedures can drastically influence result interpretation.

After completing a bianalyte SERS experiment with a reasonable number of counts, the resulting histogram should be analyzed to determine whether or not the desired threshold for SM detection has been met. This requires estimating the values of α and β for the data set. For α, there are two defined thresholds for SM detection: (1) when there is on average one molecule per spectrum and (2) when 95% of an individual analyte's SER spectra correspond to single molecules (Table 2). For β, a value close to 0.5 is highly desirable because as the detection probabilities deviate significantly from 0.5, a higher percentage of individual analyte spectra is required to prove SM detection. It should be noted, as the analyte concentrations are lowered to achieve a more rigorous threshold, the probability of locating a SM in a hotspot is also lower. Therefore, the proper threshold for SM detection should be considered on a case-by-case basis. It is critical to find a balance between selecting the most rigorous threshold while still being able to collect a reasonable number of counts. After considering all the above information, if the desirable threshold for SM detection has not been met, it may be necessary to further adjust the concentrations. We believe that through careful consideration of the factors stated above, accurate SMSERS can be achieved with bianalyte pairs.

CONCLUSION

The data presented above supports five main conclusions. First, we present a new strategy for SMSERS experiments using multiple analytes. This is an essential step toward future experiments in which chemical reactions are measured at the single molecule level and accompanied by rigorous statistical proof. Second, we quantitatively demonstrate the extent to which differences in surface binding affinities and Raman cross sections between analytes can bias the bianalyte approach for proving single molecule detection. Third, a joint Poisson-binomial model is developed to show why the bianalyte approach is compromised and discuss how to avoid these problems. Fourth, a more rigorous threshold for defining SMSERS is presented. The multianalyte studies illustrate that spectra with two or more molecules contribute non-negligibly to the spectral counts, even when at single molecule coverage. Fifth and finally, we show it is possible in SMSERS to correct for differences in analyte surface binding affinities and Raman cross sections by simply adjusting the concentration ratio between analytes, which has not been previously demonstrated. To our knowledge, we provide the first thorough guidelines for reliably proving SMSERS in future experiments. We believe appropriate implementation of these proofs will greatly advance the field of SMSERS.

ASSOCIATED CONTENT

Supporting Information

The Supporting Information is available free of charge on the ACS Publications website at DOI: 10.1021/acs.jpcc.6b00606.

Procedure for Ag nanoparticle synthesis, description of the instrumentation used for data collection, data collection scheme, histogram of peak frequencies for the 600 cm^{-1} region mode of R6G-$d_{0/4}$, additional spectra, an additional multianalyte experiment (Data Set E), a discussion on estimating β with relative signal intensities, contour plots computed from the joint Poisson-binomial model for predicting the α and β parameters, and a plot computed from the model illustrating the percentage of SM events as a function of β and α (PDF)

DOI: 10.1021/acs.jpcc.6b00606
J. Phys. Chem. C 2016, 120, 5133−5142

AUTHOR INFORMATION

Corresponding Author

*E-mail: vanduyne@northwestern.edu.

Author Contributions

The manuscript was written through contributions of all authors.

Notes

The authors declare no competing financial interest.

ACKNOWLEDGMENTS

We thank Dr. Bogdan Negru for help with MATLAB and Dr. Ash Younai for synthesizing the deuterated analytes. A.B.Z. acknowledges support from the National Science Foundation (CHE-1506683). N.L.W. acknowledges support from the Air Force Office of Scientific Research MURI (FA9550-14-1-0003) and the Department of Defense (DoD) through the National Defense Science & Engineering Graduate Fellowship (NDSEG) Program. Any opinions, findings, and conclusions or recommendations expressed in this material are those of the authors and do not necessarily reflect the views of the National Science Foundation.

REFERENCES

(1) Jeanmaire, D. L.; Van Duyne, R. P. Surface Raman Spectroelectrochemistry: Part I. Heterocyclic, Aromatic, and Aliphatic Amines Adsorbed on the Anodized Silver Electrode. *J. Electroanal. Chem. Interfacial Electrochem.* **1977**, *84*, 1−20.

(2) Stiles, P. L.; Dieringer, J. A.; Shah, N. C.; Van Duyne, R. P. Surface-Enhanced Raman Spectroscopy. *Annu. Rev. Anal. Chem.* **2008**, *1*, 601−626.

(3) Sharma, B.; Frontiera, R. R.; Henry, A.-I.; Ringe, E.; Van Duyne, R. P. SERS: Materials, Applications, and the Future. *Mater. Today* **2012**, *15*, 16−25.

(4) Cortés, E.; Etchegoin, P. G.; Le Ru, E. C.; Fainstein, A.; Vela, M. E.; Salvarezza, R. C. Strong Correlation between Molecular Configurations and Charge-Transfer Processes Probed at the Single-Molecule Level by Surface-Enhanced Raman Scattering. *J. Am. Chem. Soc.* **2013**, *135*, 2809−2815.

(5) Wilson, A. J.; Willets, K. A. Visualizing Site-Specific Redox Potentials on the Surface of Plasmonic Nanoparticle Aggregates with Superlocalization SERS Microscopy. *Nano Lett.* **2014**, *14*, 939−945.

(6) Harvey, C.; Weckhuysen, B. Surface- and Tip-Enhanced Raman Spectroscopy as Operando Probes for Monitoring and Understanding Heterogeneous Catalysis. *Catal. Lett.* **2015**, *145*, 40−57.

(7) Kneipp, K.; Wang, Y.; Kneipp, H.; Perelman, L. T.; Itzkan, I.; Dasari, R. R.; Feld, M. S. Single Molecule Detection Using Surface-Enhanced Raman Scattering (SERS). *Phys. Rev. Lett.* **1997**, *78*, 1667−1670.

(8) Nie, S.; Emory, S. R. Probing Single Molecules and Single Nanoparticles by Surface-Enhanced Raman Scattering. *Science* **1997**, *275*, 1102−1106.

(9) Fleury, L.; Segura, J. M.; Zumofen, G.; Hecht, B.; Wild, U. P. Nonclassical Photon Statistics in Single-Molecule Fluorescence at Room Temperature. *Phys. Rev. Lett.* **2000**, *84*, 1148−1151.

(10) Lounis, B.; Moerner, W. E. Single Photons on Demand from a Single Molecule at Room Temperature. *Nature* **2000**, *407*, 491−493.

(11) Treussart, F.; Clouqueur, A.; Grossman, C.; Roch, J.-F. Photon Antibunching in the Fluorescence of a Single Dye Molecule Embedded in a Thin Polymer Film. *Opt. Lett.* **2001**, *26*, 1504−1506.

(12) Michaels, A. M.; Nirmal, M.; Brus, L. E. Surface-Enhanced Raman Spectroscopy of Individual Rhodamine 6G Molecules on Large Ag Nanocrystals. *J. Am. Chem. Soc.* **1999**, *121*, 9932−9939.

(13) Weiss, A.; Haran, G. Time-Dependent Single-Molecule Raman Scattering as a Probe of Surface Dynamics. *J. Phys. Chem. B* **2001**, *105*, 12348−12354.

(14) Maruyama, Y.; Ishikawa, M.; Futamata, M. Thermal Activation of Blinking in SERS Signal. *J. Phys. Chem. B* **2004**, *108*, 673−678.

(15) Vosgröne, T.; Meixner, A. J. Surface- and Resonance-Enhanced Micro-Raman Spectroscopy of Xanthene Dyes: From the Ensemble to Single Molecules. *ChemPhysChem* **2005**, *6*, 154−163.

(16) Dieringer, J. A.; Lettan, R. B.; Scheidt, K. A.; Van Duyne, R. P. A Frequency Domain Existence Proof of Single-Molecule Surface-Enhanced Raman Spectroscopy. *J. Am. Chem. Soc.* **2007**, *129*, 16249−16256.

(17) Bizzarri, A. R.; Cannistraro, S. Levy Statistics of Vibrational Mode Fluctuations of Single Molecules from Surface-Enhanced Raman Scattering. *Phys. Rev. Lett.* **2005**, *94*, 068303.

(18) Domke, K. F.; Zhang, D.; Pettinger, B. Enhanced Raman Spectroscopy: Single Molecules or Carbon? *J. Phys. Chem. C* **2007**, *111*, 8611−8616.

(19) Le Ru, E. C.; Etchegoin, P. G. Single-Molecule Surface-Enhanced Raman Spectroscopy. *Annu. Rev. Phys. Chem.* **2012**, *63*, 65−87.

(20) Le Ru, E.; Etchegoin, P.; Meyer, M. Enhancement Factor Distribution around a Single Surface-Enhanced Raman Scattering Hot Spot and its Relation to Single Molecule Detection. *J. Chem. Phys.* **2006**, *125*, 204701.

(21) Zrimsek, A. B.; Henry, A.-I.; Van Duyne, R. P. Single Molecule Surface-Enhanced Raman Spectroscopy without Nanogaps. *J. Phys. Chem. Lett.* **2013**, *4*, 3206−3210.

(22) Blackie, E. J.; Ru, E. C. L.; Etchegoin, P. G. Single-Molecule Surface-Enhanced Raman Spectroscopy of Nonresonant Molecules. *J. Am. Chem. Soc.* **2009**, *131*, 14466−14472.

(23) Etchegoin, P. G.; Meyer, M.; Blackie, E.; Le Ru, E. C. Statistics of Single-Molecule Surface Enhanced Raman Scattering Signals: Fluctuation Analysis with Multiple Analyte Techniques. *Anal. Chem.* **2007**, *79*, 8411−8415.

(24) Le Ru, E. C.; Meyer, M.; Etchegoin, P. G. Proof of Single-Molecule Sensitivity in Surface Enhanced Raman Scattering (SERS) by Means of a Two-Analyte Technique. *J. Phys. Chem. B* **2006**, *110*, 1944−1948.

(25) Blackie, E.; Le Ru, E. C.; Meyer, M.; Timmer, M.; Burkett, B.; Northcote, P.; Etchegoin, P. G. Bi-analyte SERS with Isotopically Edited Dyes. *Phys. Chem. Chem. Phys.* **2008**, *10*, 4147−4153.

(26) Fu, Y.; Dlott, D. D. Single Molecules under High Pressure. *J. Phys. Chem. C* **2015**, *119*, 6373−6381.

(27) Kleinman, S. L.; Ringe, E.; Valley, N.; Wustholz, K. L.; Phillips, E.; Scheidt, K. A.; Schatz, G. C.; Van Duyne, R. P. Single-Molecule Surface-Enhanced Raman Spectroscopy of Crystal Violet Isotopologues: Theory and Experiment. *J. Am. Chem. Soc.* **2011**, *133*, 4115−4122.

(28) Darby, B. L.; Le Ru, E. C. Competition between Molecular Adsorption and Diffusion: Dramatic Consequences for SERS in Colloidal Solutions. *J. Am. Chem. Soc.* **2014**, *136*, 10965−10973.

(29) Andersen, P. C.; Jacobson, M. L.; Rowlen, K. L. Flashy Silver Nanoparticles. *J. Phys. Chem. B* **2004**, *108*, 2148−2153.

(30) Camden, J. P.; Dieringer, J. A.; Wang, Y.; Masiello, D. J.; Marks, L. D.; Schatz, G. C.; Van Duyne, R. P. Probing the Structure of Single-Molecule Surface-Enhanced Raman Scattering Hot Spots. *J. Am. Chem. Soc.* **2008**, *130*, 12616−12617.

(31) Pozzi, E. A.; Zrimsek, A. B.; Lethiec, C. M.; Schatz, G. C.; Hersam, M. C.; Van Duyne, R. P. Evaluating Single-Molecule Stokes and Anti-Stokes SERS for Nanoscale Thermometry. *J. Phys. Chem. C* **2015**, *119*, 21116−21124.

(32) Weber, M. L.; Litz, J. P.; Masiello, D. J.; Willets, K. A. Super-Resolution Imaging Reveals a Difference between SERS and Luminescence Centroids. *ACS Nano* **2012**, *6*, 1839−1848.

(33) Meyer, S. A.; Ru, E. C. L.; Etchegoin, P. G. Quantifying Resonant Raman Cross-Sections with SERS. *J. Phys. Chem. A* **2010**, *114*, 5515−5519.

(34) Shim, S.; Stuart, C. M.; Mathies, R. A. Resonance Raman Cross-Sections and Vibronic Analysis of Rhodamine 6G from Broadband Stimulated Raman Spectroscopy. *ChemPhysChem* **2008**, *9*, 697−699.

DOI: 10.1021/acs.jpcc.6b00606
J. Phys. Chem. C 2016, 120, 5133−5142

(35) Etchegoin, P. G.; Lacharmoise, P. D.; Le Ru, E. C. Influence of Photostability on Single-Molecule Surface Enhanced Raman Scattering Enhancement Factors. *Anal. Chem.* **2009**, *81*, 682−688.

DOI: 10.1021/acs.jpcc.6b00606
J. Phys. Chem. C 2016, 120, 5133−5142